

Vocal Folds Optical Coherence Tomography (OCT)

defined time and place for OCT analysis with voice-related biomarkers

Mette Pedersen

Pedersen, M.

MD, PhD, Ear-Nose-Throat Specialist, Head & Neck surgeon

Fellow of the Royal Society of Medicine UK

Danish Representative Union of European Phoniaticians

The Medical Center, Østergade 18, 1100 Copenhagen, Denmark

e-mail address: m.f.pedersen@dadlnet.dk

Phone: +45 31126184 www.mettepedersen.org

Member UEP Biomarkers Committee

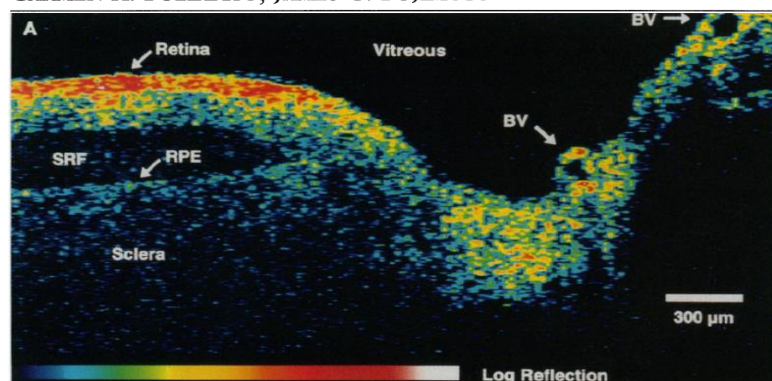
History of Optical Coherence Tomography (OCT)

- **1991**, Huang et al. described the use of OCT for *analyzing biological tissue*.
- **1997**, Tearney et al. presented in vivo images of *human tissue* with a depth of 2-3mm and a resolution of 10 μ m.
- **1997**, Sergeev et al. described the combination of OCT and *a flexible endoscope*.
- **2002**, the first commercial OCT system for ophthalmology is approved by the FDA.
- **2005**, Chen et al. demonstrated the feasibility of real-time OCT imaging in the larynx during a regular endoscopic examination in humans during anaesthesia.
- **2006**, Guo et al. presented High-Resolution OCT images of the epithelium, basement layer, and lamina propria with a prototype using a rigid 90° laryngoscope.
- **2016**, Coughlan et al. demonstrated a cross-sectional view of laryngeal vibration in vivo during phonation.

1991: Invention of OCT – ex vivo retina demonstration

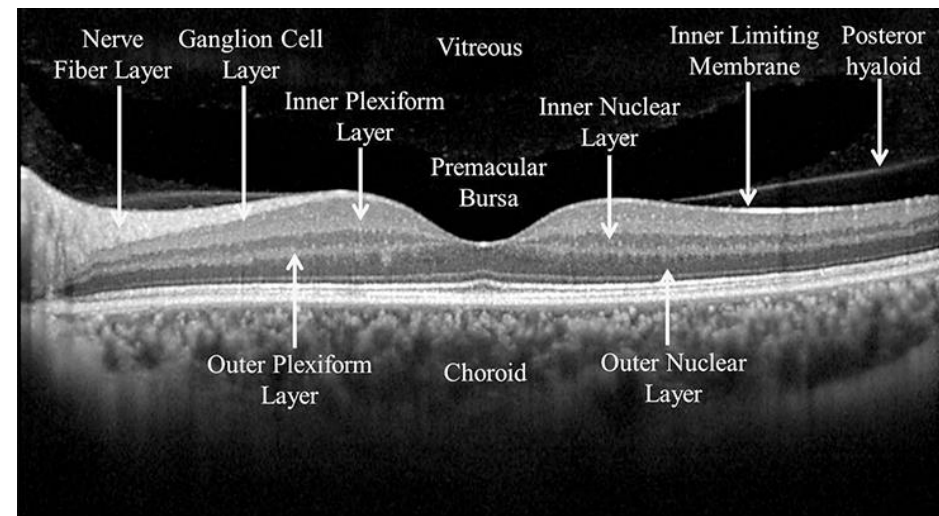
Optical Coherence Tomography

DAVID HUANG, ERIC A. SWANSON, CHARLES P. LIN,
JOEL S. SCHUMAN, WILLIAM G. STINSON, WARREN CHANG,
MICHAEL R. HEE, THOMAS FLOTTE, KENTON GREGORY,
CARMEN A. PULIAFITO, JAMES G. FUJIMOTO*



Science, New Series, Vol. 254, No. 5035 (Nov. 22, 1991), pp. 1178-1181

In vivo Images made by commercial OCT systems today



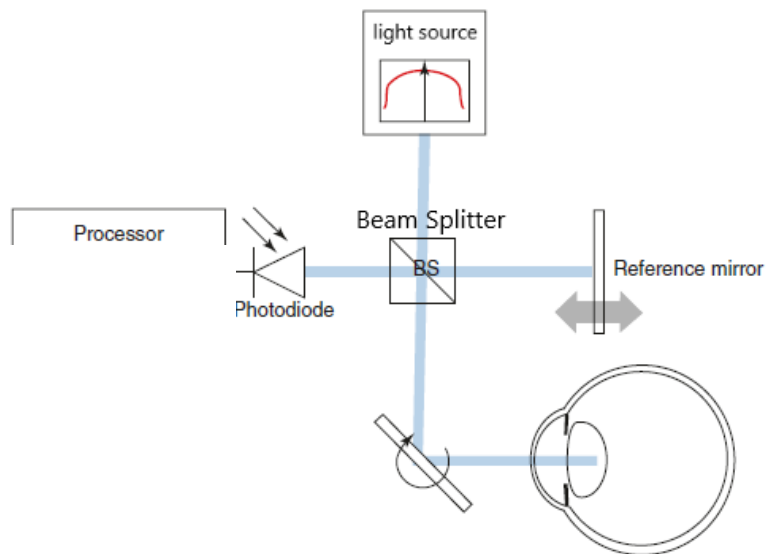
<https://en.octclub.org/normal-oct-anatomisi/>

OCT technology

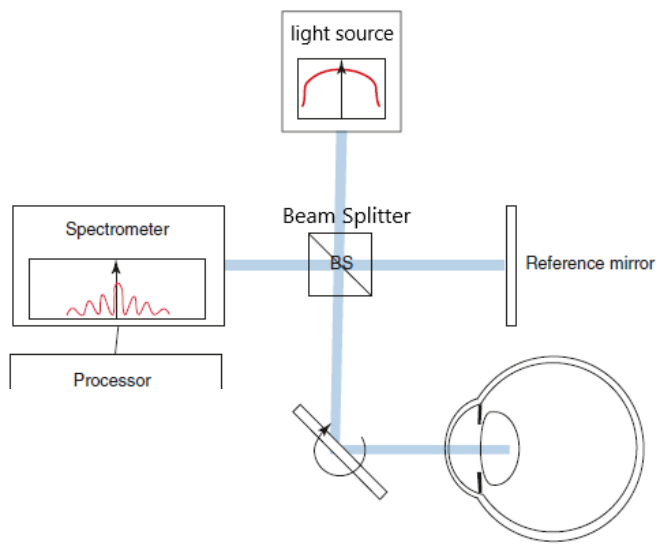
Time Domains (TD)-OCT systems were the first to be used in ophthalmology and are dependent on a moving mirror. The weak point of this technique is the need to move the reference mirror to obtain images from various depths. It creates a speed limit and can lead to motion artifacts in the scanned image.

Fourier Domain (FD)-OCT systems such as **Spectral Domain (SD)-OCT** and **Swept Source (SS)-OCT**. Both have solutions to the mirror problem. **(SD)-OCT** emits the entire needed range of wavelengths **all the time** and uses a spectrometer to decompose the signals. Whereas **(SS)-OCT** uses a tunable laser to emit the same wavelengths **in sequence and synchronizes** with the photodiode.

Time Domain (TD)-OCT



Spectral Domain (SD)-OCT



Swept Source (SS)-OCT

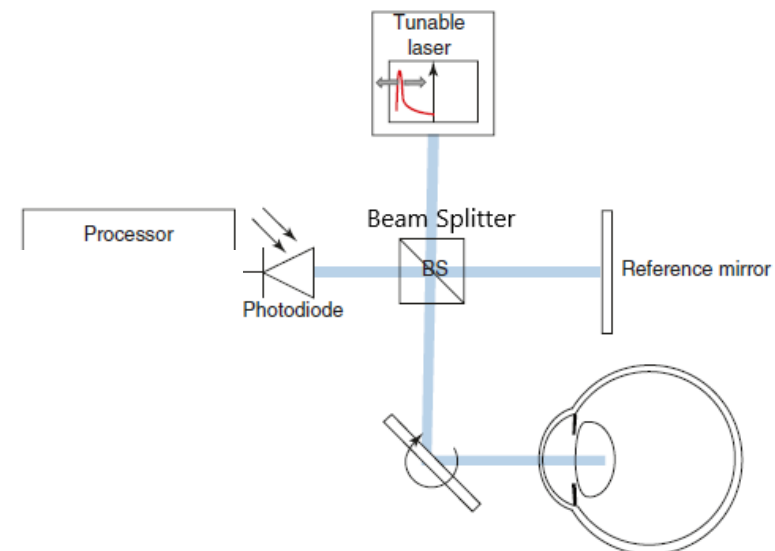


Image from: Vestri, G., Macaluso, C., Versaci, F. (2021). Anterior Segment OCT: Fundamentals and Technological Basis. In: Alió, J.L., del Barrio, J.L.A. (eds) Atlas of Anterior Segment Optical Coherence Tomography. Essentials in Ophthalmology. Springer, Cham. https://doi.org/10.1007/978-3-030-53374-8_2.

OCT domain technology

On the left side, a schematic setup of a **Time domains (TD)-OCT** system with a corresponding OCT image and histologic slide from the *lower lip*.

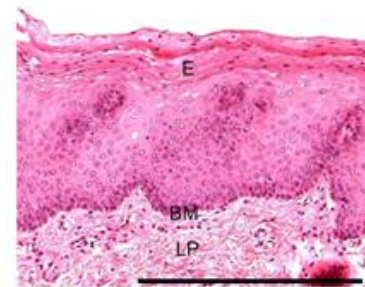
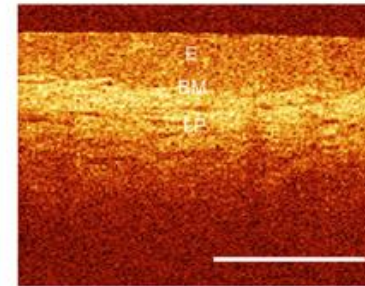
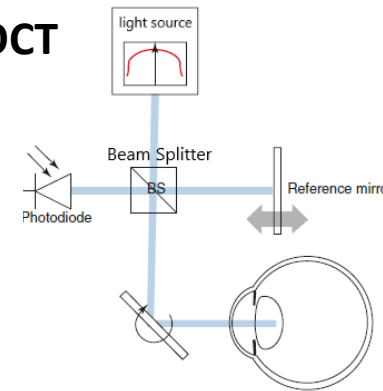
On the right, a schematic setup of a **Fourier Domain (FD)-OCT** system is depicted with a corresponding OCT image and histologic slide taken from the same spot from the *lower lip*.

The epithelial layer (E), the basement membrane (BM), and the lamina propria (LP) are clearly distinguishable on the OCT images.

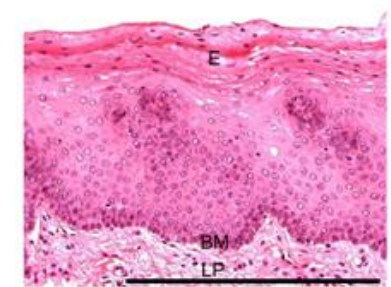
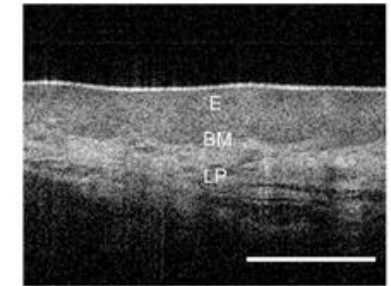
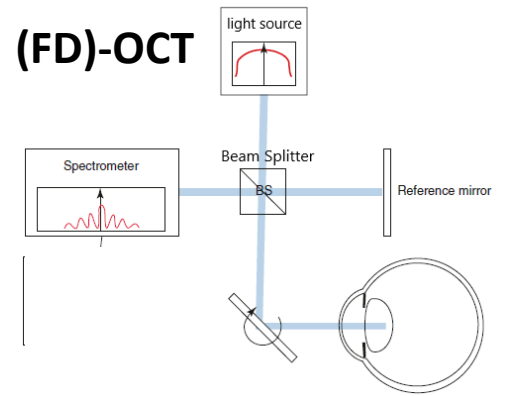
The mucosal structure of the inner lip is very similar to that of the larynx. (Scale bar shows 1 mm).

Fourier Domain (FD)-OCT is quickest because the mirror stands still.

(TD)-OCT



(FD)-OCT



Images from: Wittig, L., Betz, C., & Eggert, D. (2021). Optical coherence tomography for tissue classification of the larynx in an outpatient setting—a translational challenge on the verge of a resolution? *Translational Biophotonics*, 3(1). <https://doi.org/10.1002/tbio.20200013>.

Ultra-High-Resolution-OCT Technology at the Technical University Copenhagen Lyngby

To achieve ultra-high resolution in OCT (UHR-OCT), the following components play a significant role:

1. High-resolution *Optical Components*

To make the most of the broadband light source, the optical components (like beamsplitters, lenses, and detectors) must be optimized for the broad wavelength range of the light source (500-1.500 nm).

1. Broadband Light Source

One of the main factors that enables UHR-OCT is the use of broadband light sources. A broader bandwidth results in a shorter coherence length, which produces higher axial resolution. Common light sources are *superluminescent diodes* (SLDs).

3. Detection System

A sensitive and fast detection system is crucial for capturing the finer details in the tissue.

4. Scan System

The lateral resolution is influenced by the scanning system, especially the focusing optics. A high-quality objective lens that can focus the light to a small spot size is necessary for high lateral resolution.

To truly achieve and maintain UHR-OCT capabilities, all parts of the system need to be optimized and work synergistically.

Axial resolution is discerned between two points along or parallel to the beam path.

Lateral solution is the ability to discern between two points perpendicular to a beam path.

Rayleigh length is the distance from the waist (= at the point of its focus) to the place where the area of cross-section is doubled.

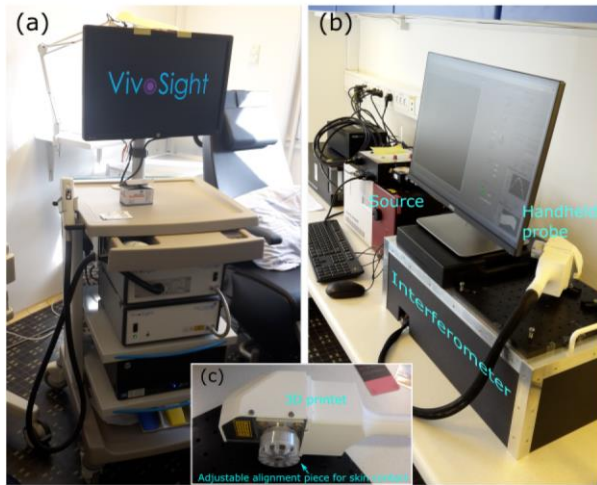
System feature	C-OCT	UHR-OCT
Operating wavelength (nm)	1305	1270 (1070-1470)
Axial optical resolution in tissue (μm)	< 5	2.2
Lateral optical resolution in air (μm)	< 7.5	6
Depth of focus (mm)	1	0.05 (Rayleigh length)
*Axial digital sampling in tissue (μm)	4.12	1.46
*Lateral digital sampling (μm)	4.41	2.93
†Scanning area (mm \times mm)	4 \times 4	3 \times 3
‡Optical average power applied (mW)	5	5

Israelsen, N. M., Maria, M., Mogensen, M., Bojesen, S., Jensen, M., Haedersdal, M., Podoleanu, A., & Bang, O. (2018). The value of ultrahigh resolution OCT in dermatology - delineating the dermo-epidermal junction, capillaries in the dermal papillae and vellus hairs. *Biomedical optics express*, 9(5), 2240–2265. <https://doi.org/10.1364/BOE.9.002240>.

Testing the dermatological Ultra-High-Resolution-OCT system for the oral cavity

As long as **probe-tissue contact** is possible, high axial and lateral resolution can be obtained:

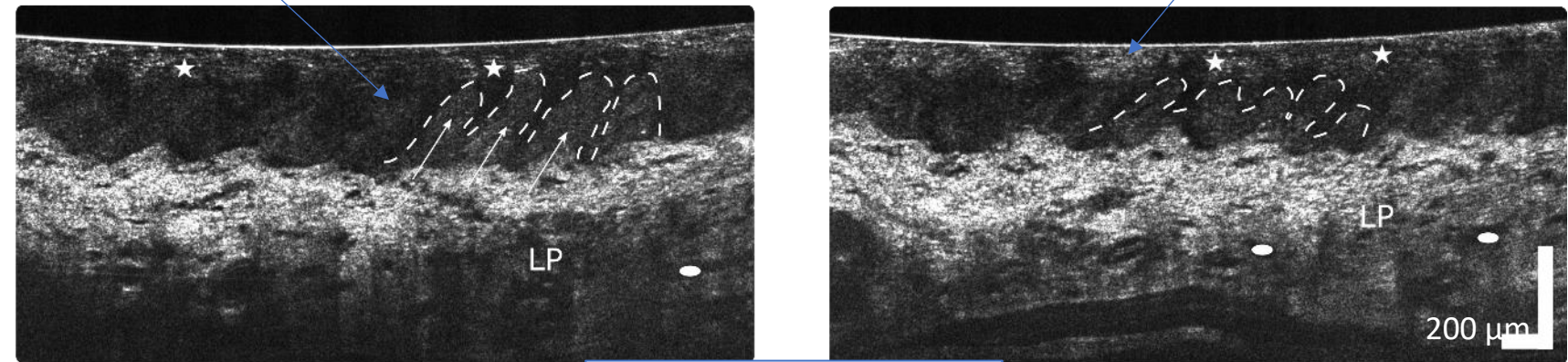
Penetration depth: 0.7 mm for UHR-OCT and 1 mm for C-OCT, respectively.



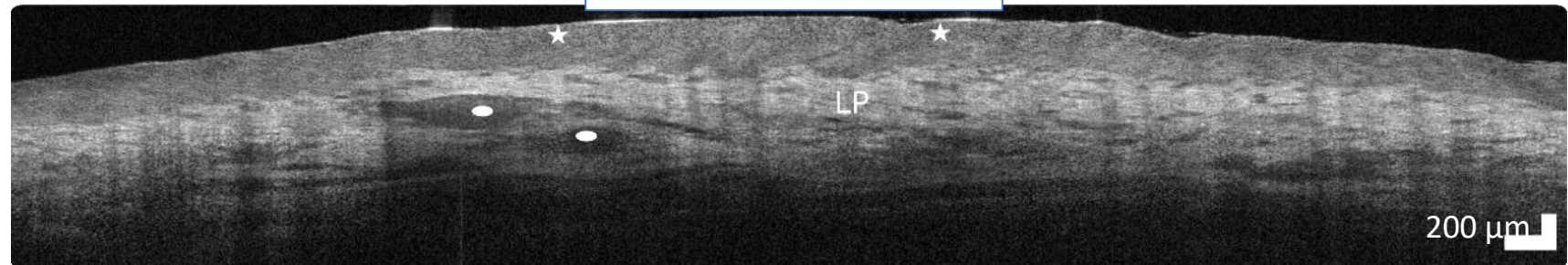
Papillae

Developed system 'UHR-OCT'

Inner lip mucosa



Commercial system 'C-OCT'

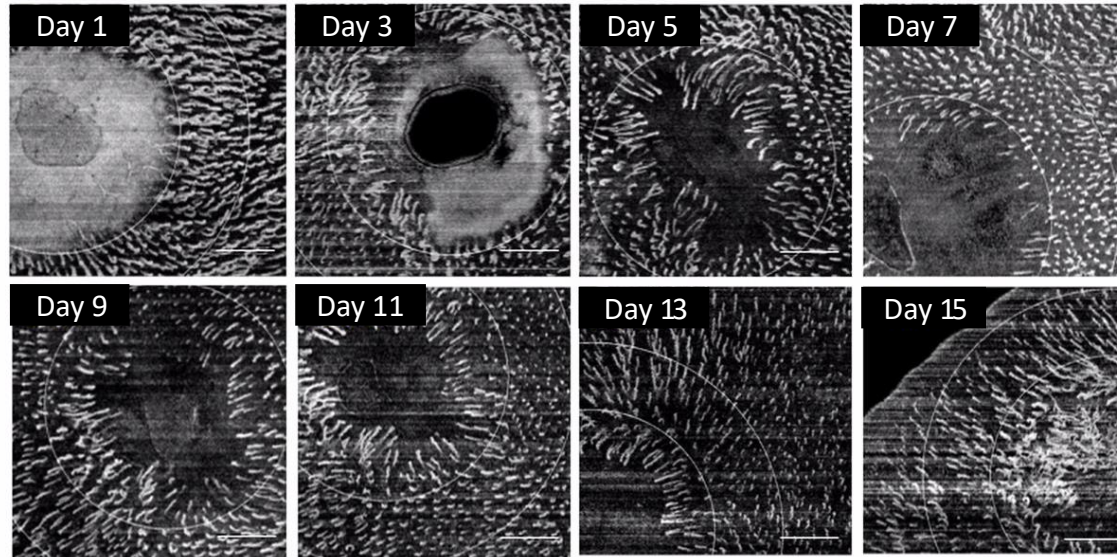


Israelsen, Niels Møller, et al. "The value of ultrahigh resolution OCT in dermatology-delineating the dermo-epidermal junction, capillaries in the dermal papillae and vellus hairs." *Biomedical optics express* 9.5 (2018): 2240-2265.

Mette Pedersen, Anders Overgård Jønsson, Mikkel Jensen, Mette Mogensen, Ole Bang, Christian F.Larsen and Niels Møller Israelsen (2022) Quantitative examination of vocal folds, perspectives for image analysis and OCT with ultra-high resolution, in part published *Ugeskr Læger* 2022;184:V02210146. Also published in part in European Voice Teachers Association (EVTA) Echo #2 - May 2023.

An example of long-ranging in vivo Swept Source Optical Coherence Tomography (SS-OCT)

- Calculation of capillary loop density ($\#/mm^2$) from day 1 to day 15 (50-100 μm)



*scale bar: 1 mm

Imaging field of view of 1600 mm^2 .

*Scale bar: 1 mm

Quantitative assessment of the vasculature network (i.e capillary loop density and vessel morphological orientations) reveals pathological and nutritional underpinnings of microcirculation for oral lesion recovery.

The progression of oral capillary angiogenesis, indicated by elevations in capillary loop density, occurs within 12 hours of disease onset and peaks at day 7 thereafter, which provides invaluable information for the time course of therapeutic treatment.



This shows the potential movement of oral cavity OCT toward clinical translations and of course UHR-OCT will optimize the findings.

Wei, W., Choi, W. J., Men, S., Song, S., & Wang, R. (2018). Wide-field and long-ranging-depth optical coherence tomography microangiography of human oral mucosa (Conference Presentation). *Proceedings of SPIE*, 16. <https://doi.org/10.1117/12.2290685>

Commercial OCT systems for vocal fold diagnostics in the future?

Lasers in Surgery and Medicine 51:412–422 (2019)

Computational Analysis of Six Optical Coherence Tomography Systems for Vocal Fold Imaging: A Comparison Study

Tiffany T. Pham, MS ^{1,2} Lily Chen, BS,¹ Andrew E. Heidari, PhD,^{1,3} Jason J. Chen, BS,^{1,3} Alisa Zhukhovitskaya, MD,^{1,4} Yan Li, MS ^{1,3} Urja Patel,¹ Zhongping Chen, PhD,^{1,3} and Brian J.F. Wong, MD, PhD^{1,2,3,4*}

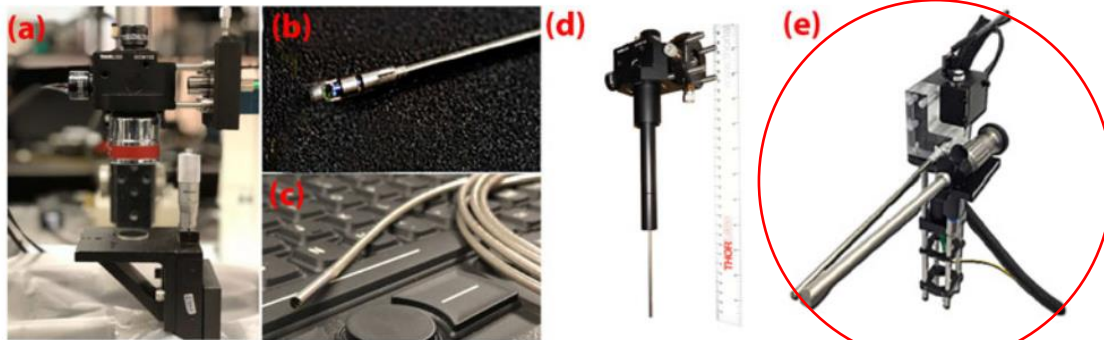
¹Beckman Laser Institute & Medical Clinic, University of California—Irvine, Irvine, California 92612

²School of Medicine, University of California—Irvine, Irvine, California 92617

³Department of Biomedical Engineering, University of California—Irvine, Irvine, California 92697

⁴Department of Otolaryngology—Head and Neck Surgery, University of California—Irvine, Orange, California 92868

No.... But a number of endoscope OCT systems have been developed:



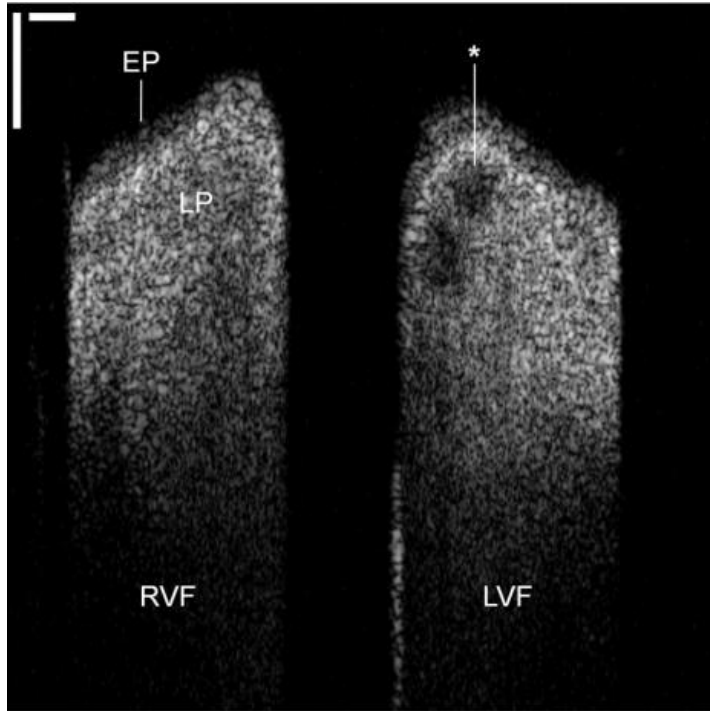
Endoscopes: a-e

TABLE 1. Specifications of OCT Systems

OCT system type, center wavelength, A-line rate	Probe type	Working distance	Axial resolution	Lateral resolution	Pixel resolution	Imaging speed
SS-OCT, 1310 nm, 200 kHz VCSEL	Microscope scanner	35 mm	5.8 μm	22.5 μm	3.8 μm	200 fps
SS-OCT, 1700 nm, 90 kHz	Microscope scanner	35 mm	12 μm	29.2 μm	8.5 μm	90 fps
SS-OCT, 1310 nm, 50 kHz	Flexible side viewing rotational endoscope	7 mm	10 μm	102 μm	4.8 μm	50 fps
TD-OCT, 1310 nm, 254 Hz	Flexible forward viewing endoscope	1.6 mm	15 μm	25 μm	6.9 μm	1 fps
SS-OCT, 1310 nm, 50 kHz	Rigid forward viewing endoscope	8.5 mm	9.8 μm	5.4 μm	4.8 μm	50 fps
SS-OCT, 1310 nm, 200 kHz VCSEL	Rigid side viewing endoscope	7-10 cm	9.3 μm	100 μm	5.9 μm	200 fps

SS-OCT, swept-source OCT; VCSEL, vertical-cavity surface-emitting laser; fps, frames per second; TD-OCT, time-domain OCT.

Cross-sectional OCT image of the vocal folds in the coronal plane

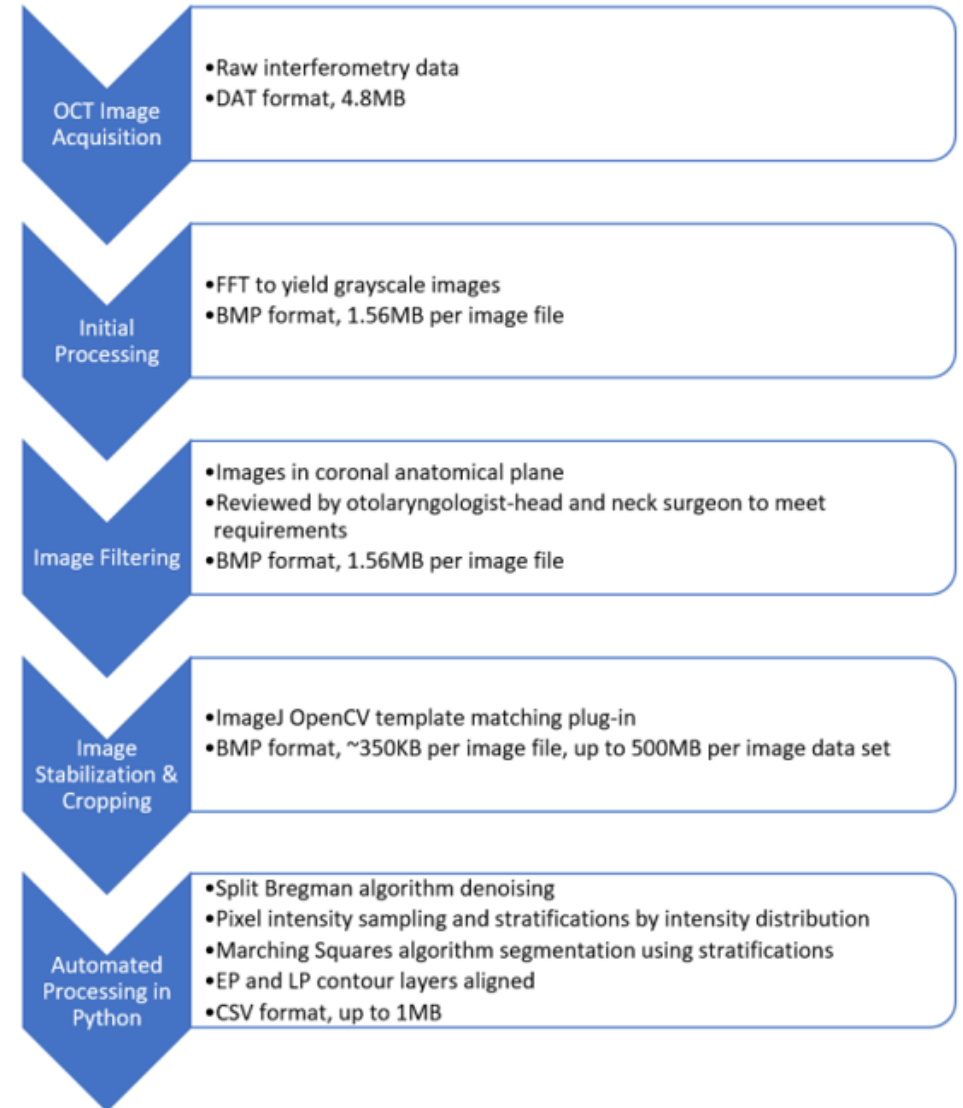


This is a OCT coronal plane with subepithelial lesion on a single frame. The cross-sectional OCT image of the vocal fold depicts a subepithelial hypodensity (asterix).

The scale bars denote 500 μm axially and laterally; Scaling was adjusted for EP, epithelium; and LP, lamina propria. right and left vocal folds.

SHARMA, G. K. et al. Surface kinematic and depth-resolved analysis of human vocal folds in vivo during phonation using optical coherence tomography. *Journal of biomedical optics*, [s. l.], v. 26, n. 8, 2021.

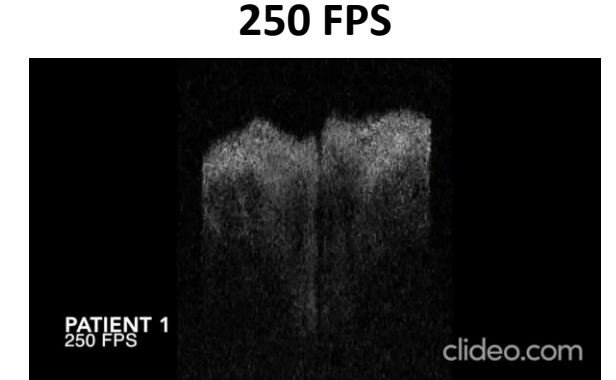
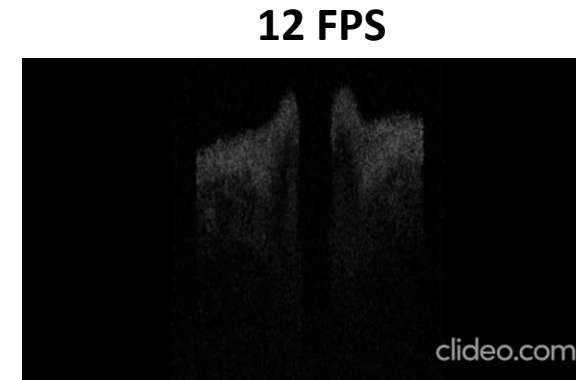
A flowchart representative of initial image processing steps is presented. Major steps and the respective resulting data set and format are indicated.



Cross-sectional OCT

Cross-sectional OCT images of the Vocal folds in the coronal plane, with delineation of superficial VF layers.

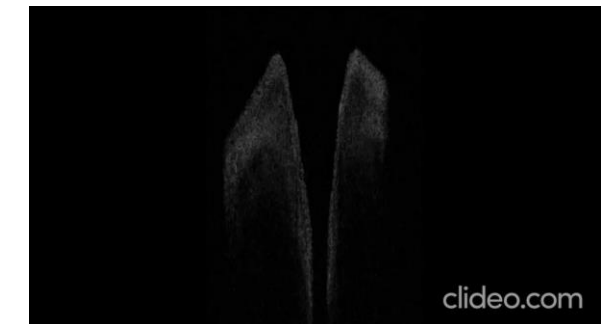
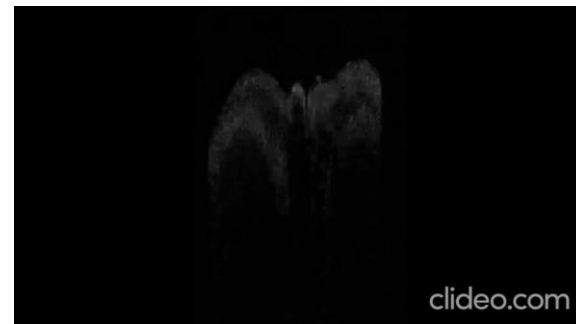
Patient 1



Patient 2

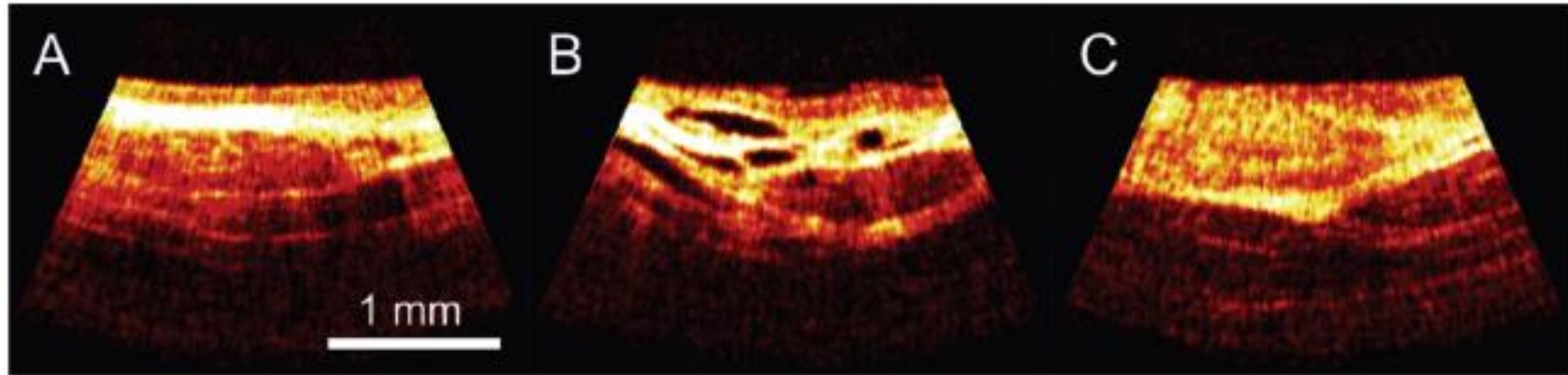


Patient 3



SHARMA, G. K. et al. Surface kinematic and depth-resolved analysis of human vocal folds in vivo during phonation using optical coherence tomography. Journal of biomedical optics, [s. l.], v. 26, n. 8, 2021

OCT images of the pharynx mucosa



OCT images of healthy mucosa of the pharynx, and hypertrophic pharyngitis before and after therapy.

A: Normal:

- ❖ The upper layer is characterized by a moderate signal level corresponding to stratified squamous epithelium,
- ❖ while the lower layer with a high signal level corresponds to lamina propria with a high content of elastin fibers.
- ❖ In the submucous layer glands and lymphoid elements are manifested in OCT images by irregularly shaped areas of different sizes and signal levels.

B: Chronic pharyngitis:

- ❖ Catarrhal form of chronic pharyngitis, a persistent diffuse congestion of the veins accompanied by pronounced edema of tissues is observed leading to the disintegration of morphological structures and an increase in the volume of lymphoid tissue.
- ❖ Chronic pharyngitis has a mixed form, in this case, the morphological features of hypertrophic pharyngitis can be observed in the background of changes typical for a catarrhal form of the disease, for example, formation of cysts, in the subepithelial cystic expansions, bulbs and “bights”

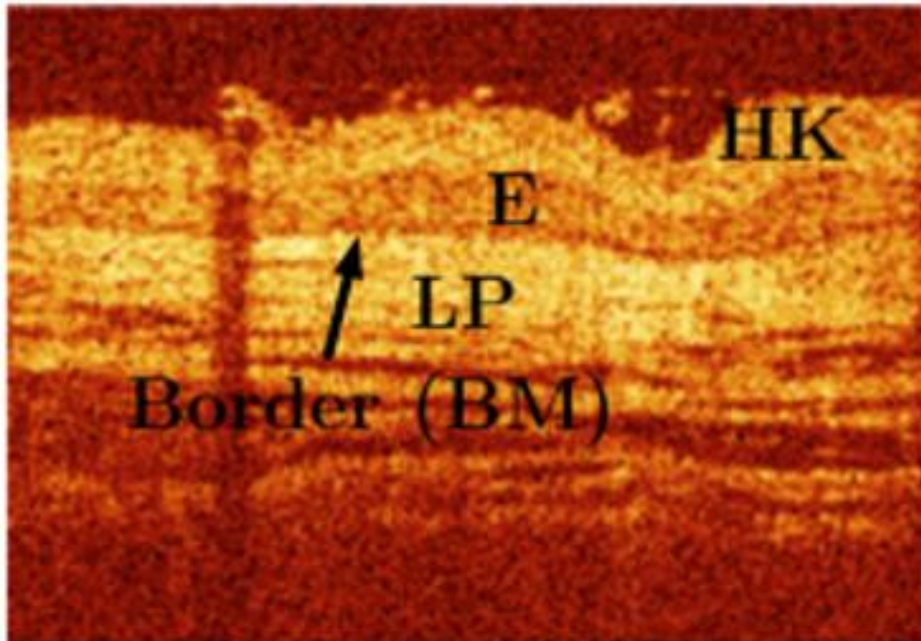
C: After therapy

- ❖ Therapy is accompanied by water crystallization manifested in OCT images by the disappearance of low-signal areas and a balance of the signal level in the upper layers.

OCT pictures and Deep Learning for cancer detection

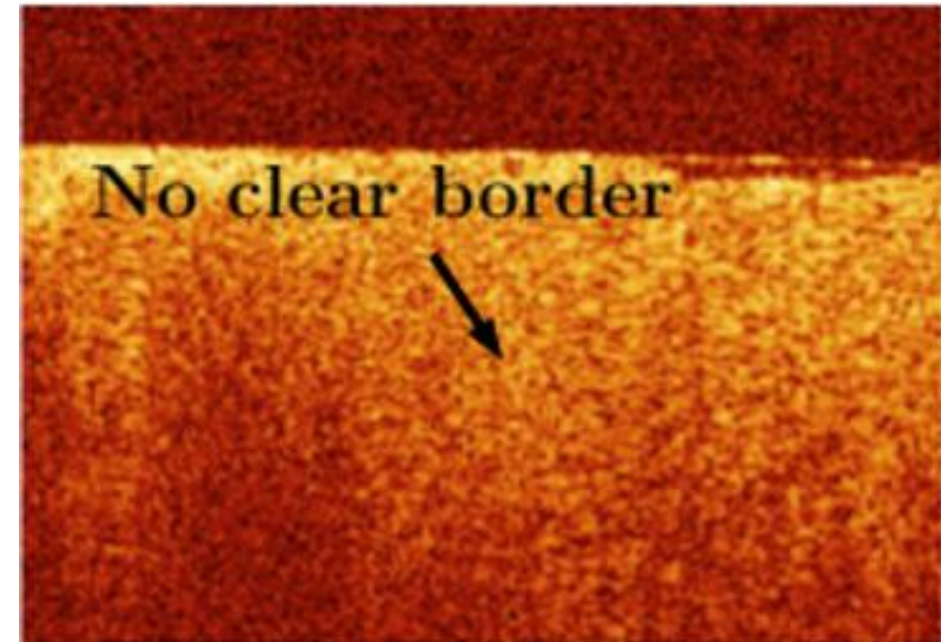
Left: hyperkeratotic lesion at the floor of the mouth.

- ❖ BM – Basement Membrane
- ❖ LP – Lamina Propria
- ❖ E – Epithelial layer
- ❖ HK – Hyperkeratosis



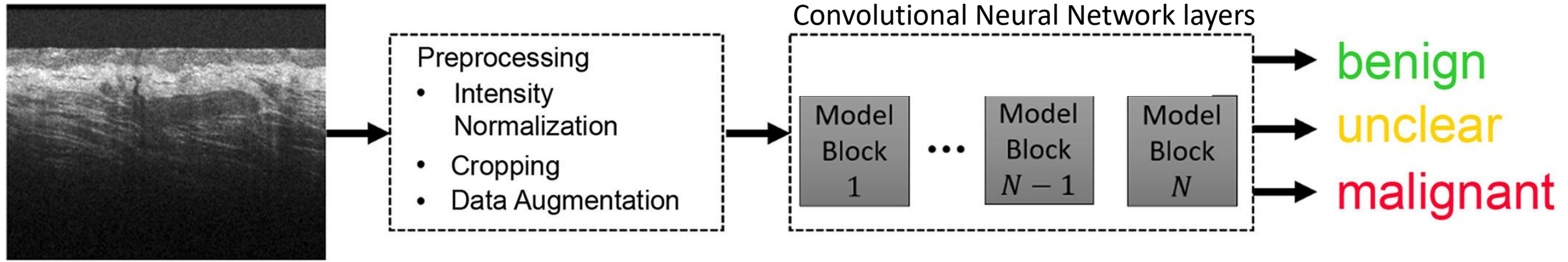
Right: Invasive lesion at the floor of the mouth.

- ❖ No Clear border between epithelial layer and LP



The Oct finding was treated with deep learning models Resnet18, Densenet121, and SE-ResNeXt50 were used. These were pre-trained on ImageNet for transfer learning which has been successful for OCT classification tasks.

artificial intelligence of Deep Learning for cancer detection (continued)



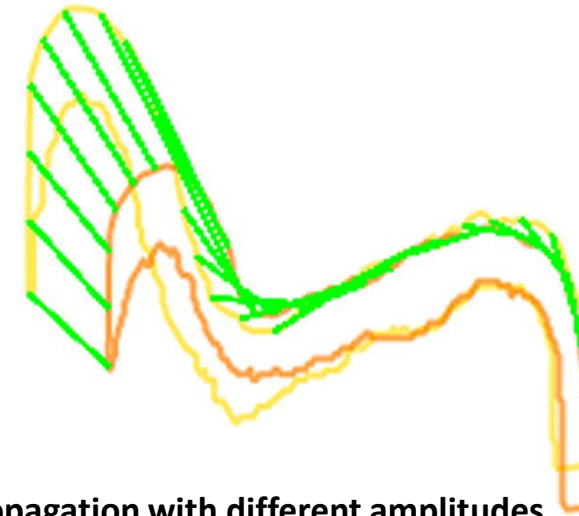
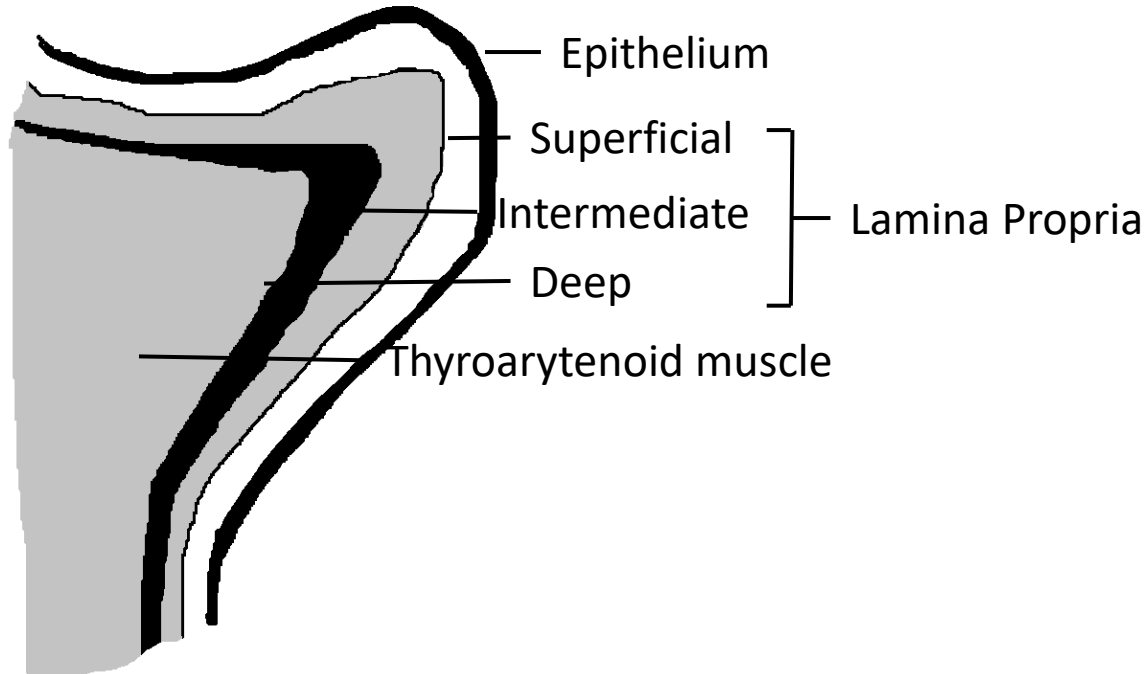
The pictures shows a deep learning workflow for automated tissue classification in OCT images:
The OCT image or video is first preprocessed and then analyzed by deep learning techniques.

The final output could classify the tissue into different groups supporting the physician's decision:
benign (no further action is needed), *malignant* (a surgical resection should be performed soon), *unclear* (further investigations are needed)

This is where voice-related biomarkers really make a difference because place and time of the measure is described

Vocal fold mucosa propagation as a measure of function.

The vertical displacement was in males 1.38 and in females 1.24 μm



Propagation with different amplitudes.

For the X-axis horizontal wave: 30 points were distributed equidistantly along the width of the superior contour of each vocal fold.

For the Y-axis vertical wave: with consecutive phonation over a period of at least 3 s, the vertical mucosal wave can be visualized and measured.

The Green lines visually demarcate the displacement vector between the 30 equidistant points along the superior surface of each segmentation.

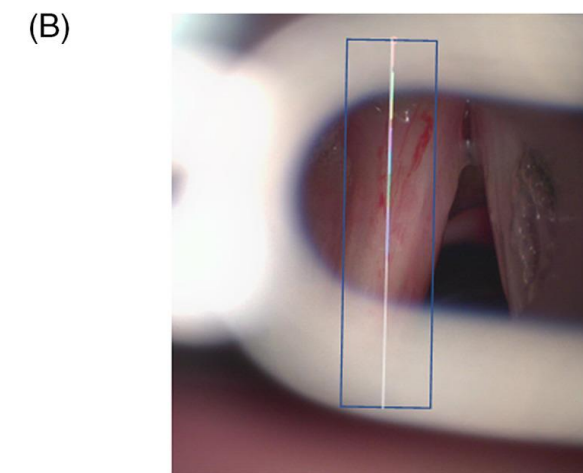
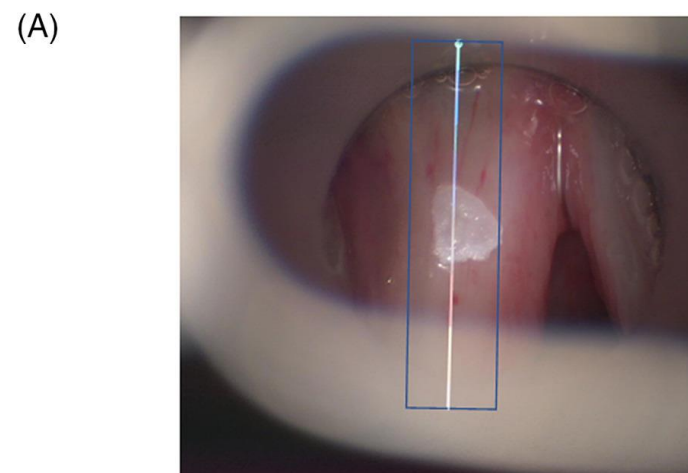
The Yellow and orange lines show two epithelium segmentations from consecutive image frames.

During resting state, in males the epithelium state was $106 \pm 49 \mu\text{m}$, and the lamina propria $367 \pm 197 \mu\text{m}$
in females it was $66 \pm 24 \mu\text{m}$ and $595 \pm 179 \mu\text{m}$ respectively.

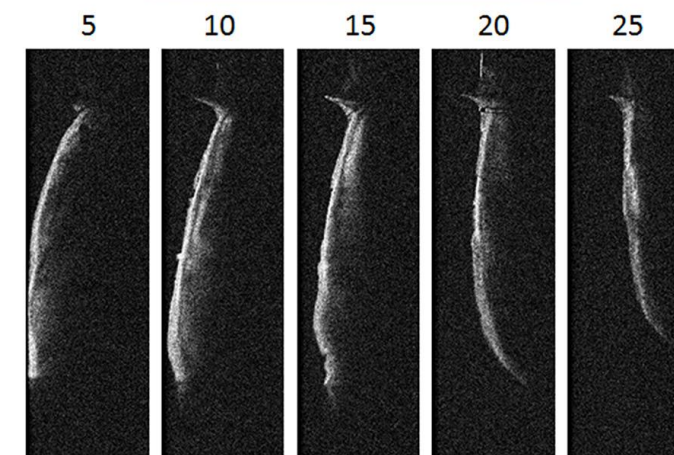
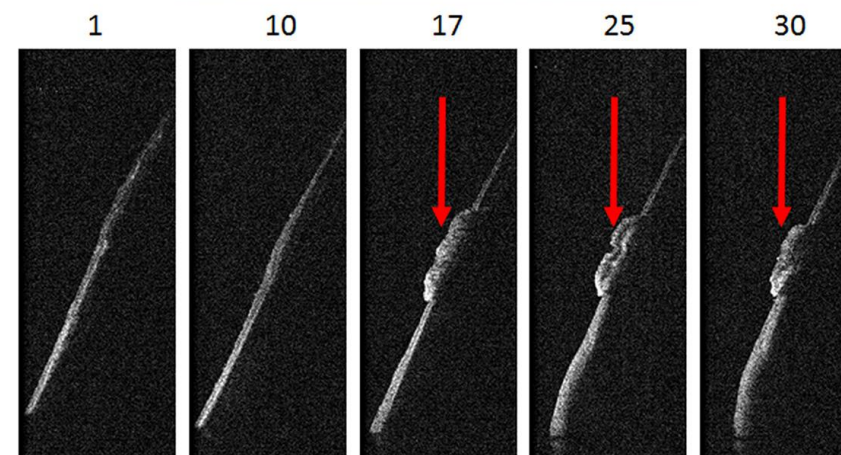
During phonation in males the epithelium state was $81 \pm 35 \mu\text{m}$, and the lamina propria $376 \pm 130 \mu\text{m}$
in females it was $79 \pm 38 \mu\text{m}$ and $522 \pm 220 \mu\text{m}$ respectively.

OCT images of a hyperkeratotic lesion of the left vocal fold operated in vivo in an outpatient

(A)
the vocal fold before laser ablation with the corresponding OCT image slides taken from lateral (1) to medial (30) clearly depicting the thickening of the epithelium (17, 25, 30) **as indicated by the red arrow.**

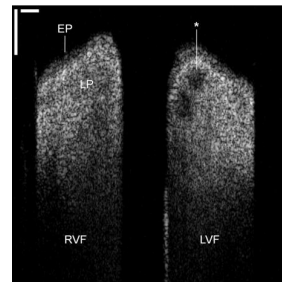


(B)
the vocal fold after laser ablation with corresponding OCT image slides, taken from lateral (5) to medial (25) depicting a smooth epithelial surface.



Conclusion

- Optical coherence tomography (OCT) can provide 3D microscopically detailed sub surface images 0.5-2 mm in-depth of larynx mucosa tissue composition.
- Quantitative measuring of the moving vocal folds has been demonstrated.
- No commercial OCT systems for imaging vocal folds exist (in contrast to ophthalmology)
- Various probes for the larynx have been developed – technology is there!
- **The problem of precise time and place of client measurement can be defined much better with voice-related biomarkers.**



Thank you for listening